ACS OMEGA

Article

Cite This: ACS Omega 2019, 4, 9181−9187

http://pubs.acs.org/journal/acsodf

Nitric Oxide Uncaging from a Hydrophobic Chromium(III) PhotoNORM: Visible and Near-Infrared Photochemistry in Biocompatible Polymer Disks

Po-Ju Huang,[†,‡] John V. Garcia,[†,‡] Aidan Fenwick,[†,‡] Guang Wu, and Peter C. Ford*

Department of Chemistry and Biochemistry, University of California, Santa Barbara, Santa Barbara, California 93106 United States

Supporting Information

ABSTRACT: Devices consisting of polymer disks (PDs) of optically clear or translucent, medical-grade silicone loaded with a new hydrophobic, oxygen-stable, photoactivated nitric oxide-releasing moiety (photoNORM) are described. The photoNORM is the new *O*-nitrito chromium(III) complex *trans*-[Cr(PetA)$(ONO)_2$](BF_4) (PetA = 5,14-dimethyl-7,12-diphenyl-1,4,8,11-tetraaza-cyclotetradecane), of which the synthesis, X-ray crystal structure, and solution-phase photochemistry are described. Several different commercially available silicone polymers were tested with this photoNORM, and nitric oxide photouncaging with 451 nm light from these systems is compared. In addition, PDs were loaded with the photoNORM and neodymium-sensitized upconverting nanoparticles (Nd-UCNPs). The Nd-UCNPs absorb NIR light at ∼800 nm and activate NO release from the *trans*-$[Cr(PetA)(ONO)_2]^+$ cation. The use of such ensembles as implants provides a potential strategy for the in vivo uncaging of NO at physiological targets triggered by tissue-transmitting NIR excitation. Also reported are the X-ray crystal structures of *cis*- and *trans*-{Cr(PetA)Cl_2]Cl.

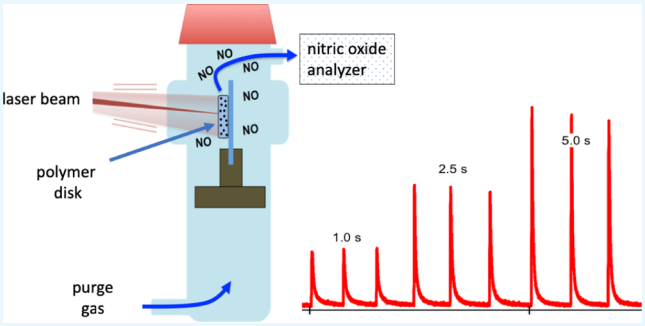

INTRODUCTION

There has been considerable recent interest in developing strategies for photolysis-induced release (photouncaging) of various bioactive small molecules at physiological targets for potential therapeutic applications.[1−11] One such molecule is the promiscuous bioregulator nitric oxide (NO), which plays important roles in mammalian cardiovascular and neurobiology as well as immune response[12,13] and which, among other properties, displays antibacterial activity in combating biofilms.[14] This combination has drawn attention from this laboratory[15−17] and others[18−25] to the design and study of photoactivated NO-releasing moieties (photoNORMs). The advantages of photouncaging include exquisite control of the timing, location, and dosages of delivery. However, two disadvantages come immediately to the forefront. The first is the difficulty in localizing the caged bioactive molecule at the desired target area, where release can be triggered with light. The other is the rather poor transmission of ultraviolet and visible wavelengths through mammalian tissue with the exception of the relatively narrow window falling at long visible and shorter near-infrared (NIR) wavelengths.[26] Not only do shorter wavelengths penetrate poorly but the resulting tissue heating from the absorption of these wavelengths can also lead to collateral damage.

One approach to targeted placement at a specific site is to incorporate the bioactive compound into a solid matrix (for example, a biocompatible polymer) that can be used as an implant.[27−30] Implants are already used for timed drug release,[31] but one using a caged precursor allows release only upon demand and provides dosage control by the amount of light used.[32] Such a device could be attached to an optical fiber that would transmit light to the target site to uncage the desired bioactive molecule. Alternatively, if the device were responsive to NIR excitation, then the use of the fiber and associated hardware may be unnecessary.

In this context, we previously described devices consisting of mm-sized poly(dimethylsiloxane) (PDMS) polymer disks (PDs) containing upconverting nanoparticles (UCNPs) and infused with Roussin's black salt $Na[Fe_4S_3(NO)_7]$ (RBS).[33] UCNPs serve as antennas to effect NIR-to-visible (or UV) upconversion by sequential multiphoton excitation at 980 nm with the lanthanide ion Yb^{3+} as the light-absorbing sensitizer and a second lanthanide ion (Er^{3+} or Tm^{3+}) as the emitter of visible and/or UV wavelengths after energy transfer from the sensitizer.[34−38] The upconverted light emitted from the UCNPs was reabsorbed by the RBS, leading to photoinduced NO release from this photoNORM.[39] The advantage of UCNPs is that upconversion requires much lower-excitation intensities than does simultaneous two-photon excitation; so, one can use a relatively simple diode laser operating at 980 nm to effect multiphoton excitation of the UCNPs leading to NO release.[34] Furthermore, we demonstrated that NIR excitation

Received: March 2, 2019
Accepted: May 7, 2019
Published: May 24, 2019

DOI: 10.1021/acsomega.9b00592
ACS Omega 2019, 4, 9181−9187

Scheme 1. Synthetic Sequence Used To Prepare *Trans*-[Cr(PetA)(ONO)$_2$]BF$_4$[a]

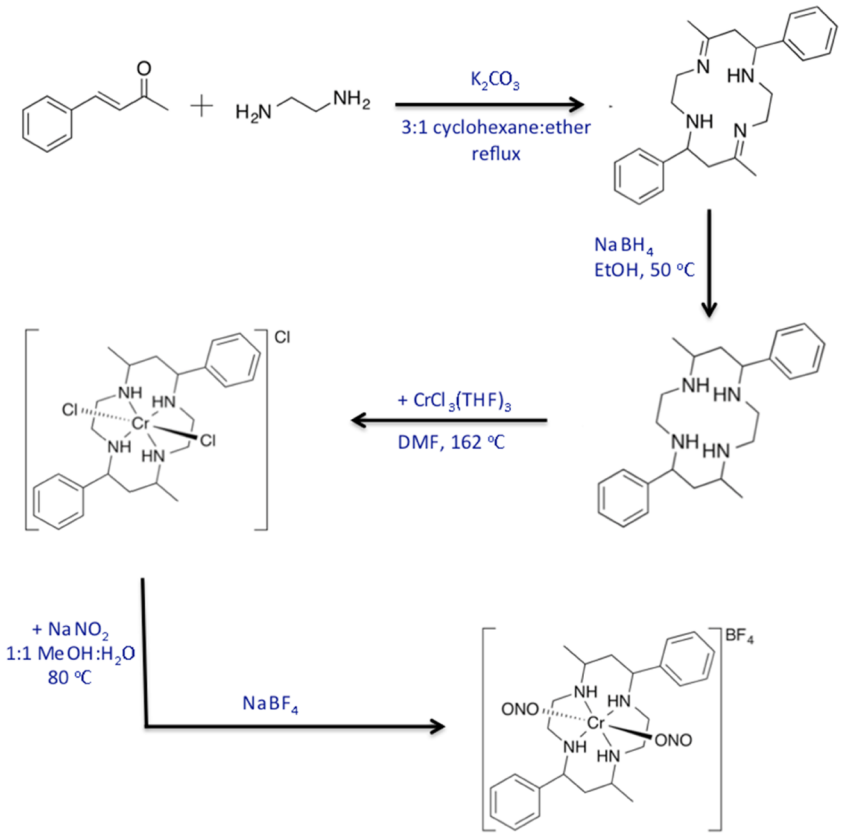

[a]See the SI for more details.

triggered photouncaging from these RBS-containing devices even through tissue filters.[33]

Described here is an investigation of analogous devices based on PDs prepared from a series of different commercially available, medical-grade, biocompatible silicone polymers with the goal of evaluating whether different formulations would affect the photochemical uncaging of NO. The photoNORM selected in these studies is the BF_4^- salt of the previously unreported chromium(III) complex cation *trans*-[Cr(PetA)(ONO)$_2$]$^+$ (PetACrONO), where PetA = 5,14-dimethyl-7,12-diphenyl-1,4,8,11-tetraazacyclotetradecane, the synthesis of which is described. The PetACrONO salt is photoactive toward NO release in solution, is hydrophobic, and is readily infused into PDs prepared from these polymers. Nitric oxide uncaging from the resulting devices can be activated by visible light excitation.

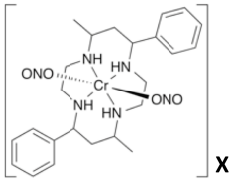

[*trans*-Cr(PetA)(ONO)$_2$]X

PetACrONO

Also described are PDs prepared both with PetACrONO and with this photoNORM and neodymium(III)-doped β-NaYF$_4$:Tm/Nd/Yb/Gd@NaYF$_4$:Nd-UCNPs (Nd-UCNPs).[40,41] The advantage of Nd-UCNPs is that these can be excited with a continuous NIR diode laser operating at ~800 nm[42,43] and the resulting upconverted visible light is reabsorbed by the photoNORM to uncage NO. Excitation at ~800 nm allows one to avoid the modest absorbance by water at 980 nm, thereby improving NIR transmission depth and reducing potential tissue damage due to heating effects. During the course of the experiments described here, Ostrowski and co-workers[30] reported the NIR-induced release of NO from several polysilicone composites containing the well-studied[44,45] photoNORM *trans*-[Cr(cyclam)(ONO)$_2$]X ("CrONO", cyclam = 1,4,8,11-tetraaza-cyclotetradecane, X$^-$ = BF_4^- or BPh_4^-) and UCNPs that are activated by visible and 980 nm excitation.

EXPERIMENTAL SECTION

Materials. The NaYF4:Yb/Tm/Nd/Gd (30/0.5/1/20 mol %)@NaGdF4:Nd (20 mol %) core−shell UCNPs (Nd-UCNPs) used in these studies were provided by Dr. E. M. Chan and E. S. Levy at the Molecular Foundry of the Lawrence Berkeley National Laboratory. The biocompatible silicone polymers used included NuSil Technology LLC formulations MED-4805, MED4-4220, MED-6019, MED-6215, MED-6233, and MED-6755. The NuSil silicones were gifts from the Allergan Corporation and NuSil Technology LLC.

Syntheses. The synthesis of the PetACrONO salts is outlined in Scheme 1. The ligand PetA was prepared by the $NaBH_4$ reduction of the unsaturated macrocycle 5,14-dimethyl-7,12-diphenyl-l,4,8,11 tetraazacyclotetradeca-4,14-diene, as described by Hideg and Lloyd.[46] The dichloro Cr(III) complex *trans*-[Cr(PetA)Cl$_2$]Cl was prepared by the reaction of PetA and $CrCl_3(THF)_3$ in refluxing dimethylfor-

DOI: 10.1021/acsomega.9b00592
ACS Omega 2019, 4, 9181−9187

mamide, as described by DeRosa for analogous macrocycles.[47] This procedure gives a mixture of the *cis*- and *trans*-complexes, which was separated by chromatography on silica. For the reaction with PetA, the latter is favored (70% yield) over the less desirable *cis* form (10%), which could be converted to the *trans* form by refluxing in dichloromethane (DCM). The bis(*O*-nitrito) complex salt *trans*-[Cr(PetA)$(ONO)_2$]BF_4 was synthesized from *trans*-[Cr(PetA)Cl_2]Cl by procedures modified from those described for the cyclam analogues (Scheme 1).[43] Synthesis details and analytical data are reported in the Supporting Information (SI).

X-ray Crystallography. The solid-state crystal structures of *trans*-[Cr(PetA)$(ONO)_2$]BF_4 and of *cis*- and *trans*-[Cr(PetA)Cl_2]Cl were determined by X-ray diffraction on a Kappa Apex II single-crystal diffractometer. X-ray structural data are summarized in SI Tables S1−S3.

Preparation and Loading of Polymer Disks. Procedures similar to those described previously[33] were used. The round PDs (10 mm diameter, 2 mm thick) were fabricated by mixing the monomer base (Part A) and the curing agent (Part B) in the weight ratios recommended by data sheets from the manufacturer NuSil Technology for the different formulations and then deaerated under vacuum in the antechamber of an inert atmosphere box for 25 min. An aliquot of this mixture (∼200 μL) was added to a custom-made mold (10 mm diameter, 2 mm height). Next, the PD was annealed at ∼110 °C for ∼1 h and then allowed to set at room temperature for at least 12 h. After fabrication, the PDs were removed from the mold and transferred into the glovebox for infusion of the photoNORM. This was done by incubating the PD in a concentrated tetrahydrofuran solution (0.4 mL) of *trans*-[Cr(PetA)$(ONO)_2$]BF_4 (3.1 mg/mL) for 5 h followed by vacuum drying. This was repeated 3 times. Finally, the dried PDs were washed with THF and methanol and multiple times with water to remove surface photoNORM that was not impregnated into the PD. This was repeated until no PetACrONO was detected in the wash solution. After several such washes, no leaching was evident in the solution spectra even after 24 h incubation in aqueous media. The resulting PDs were stored in the dark under an inert atmosphere until use. For PDs prepared for NIR studies, a 5 mg portion of the solid Nd-UCNPs was physically mixed with the polymer in the disk molds before curing.

The loading efficiency was analyzed by ICP-MS. The PDs were digested in a 5 mL volume of a 1 M ammonium tetrafluoroborate solution in THF for 5 days. The solutions were then heated at 50 °C to evaporate the THF, and the resulting oils were further digested in concentrated nitric acid for 2 days. The nitric acid was then removed by heating, and the resulting solution was redissolved into a 2% nitric acid solution. Analysis was carried out using an Agilent 8800 Triple Quadrupole ICP-MS calibrated against a chromium standard. Although there was some variation from disk to disk, the loading efficiency, after washing, fell in the range of 65−97% (82% ave.) of the initial PetACrONO available.

Photochemical Studies. *Solution-Phase Studies.* Photolysis of PetACrONO was carried out in isobutyronitrile solution. The NO release was determined by entraining the photolysis solution contained in a "Y" cell with medical-grade air, which then flowed to a Sievers Nitric Oxide Analyzer (NOA, GE model NOA-280i), where it was detected and quantified via a calibrated chemiluminescence technique (SI Figure S1). (In each case, the entraining gas was purged through a solvent bubbler prior to entering the photolysis cell to reduce evaporative losses.) The photoexcitation source was either the 365 nm emission from a 200 W high-pressure mercury lamp isolated with an interference filter or the 451 nm light from a Luxeon blue light-emitting diode (LED) (SI Figure S2). Excitation intensities at 365 nm were determined by ferrioxalate actinometry,[47] while those at 451 nm were determined with a power meter (Newport model 8442 PE). Excitation intervals were controlled using a Uniblitz shutter, and quantum yields of NO release (Φ_{NO}) were determined by evaluating the NO released and recorded using the NOA software ("Liquid") for varied excitation intervals. The slope of a plot of NO released vs total light absorbed by the solution gives Φ_{NO} (SI Figure S3).

Photoreactions in Polymer Disks. The PDs were attached to a glass substrate using a double-sided tape that was then mounted into a flow cell where the photolysis was effected under streaming helium or medical-grade air (SI Figure S1).[32] The NO released from the sample was transferred from the cell via the flowing gas to the NOA, where it was detected and quantified. The visible photoexcitation source was the royal blue (451 nm) Luxeon LED operating in the 45−500 mW range. The NIR photoexcitation source (794 nm) was a Sheaupac NIR fiber-coupled diode laser module from ILX Lightwave. Incident photon flux during photolysis was measured using a Newport model 8442 PE optical power meter with a silicon photodiode detector. The photolysis laser beam (0.8 mm diameter) was oscillated by reflecting of two movable mirrors controlled by a Tektronix AFG320 arbitrary function digital generator, as described previously (SI Figure S4).[32] The two mirrors each control the scanning width in one direction (horizontal or vertical) so that adjusting the individual oscillating frequencies defines the size of the scanned area. Experiments were run with mirror frequencies of 78.93 and 48.93 Hz, which scanned the collimated laser beam over most of the 10 mm diameter PDs to compensate for inhomogeneities in Nd-UCNP distribution in the polymer matrices while avoiding the damage that sometimes occurred when focusing on a single spot.[32] Excitation intervals were controlled by the Uniblitz shutter.

RESULTS AND DISCUSSION

Syntheses and Structures of *Trans*-[Cr(PetA)Cl_2]Cl and *Trans*-[Cr(PetA)$(ONO)_2$]BF_4. Scheme 1 illustrates the sequence used to prepare these two new compounds. The cis-dichlorido complex *cis*-[Cr(PetA)Cl_2]Cl is an isolable minor byproduct of the synthesis of the *trans*-analogue (see the Supporting Information for more details). The X-ray crystal structure of the *trans*-Cr(PetA)$(ONO)_2^+$ cation is displayed in Figure 1, and the unit cell structure of the *trans*-[Cr(PetA)$(ONO)_2$]BF_4 salt is shown in SI Figure S5. The unit cell structure of *trans*-[Cr(PetA)Cl_2]Cl is shown in SI Figure S6. Data (crystal and structural refinement data, atomic coordinates plus bond lengths and angles) from the crystal structure determinations of these two compounds and for *cis*-[Cr(PetA)Cl_2]Cl are summarized, respectively, in SI Tables S1−S3. The Cl−Cr−Cl angles for the *cis*- and *trans*-dichlorido complexes are 88.8 and 180.0°, respectively. The electronic spectrum of PetACrONO is shown in Figure 2.

Solution-Phase Photochemical Reactions. The solution-phase photolysis of *trans*-[Cr(PetA)$(ONO)_2$]BF_4 was examined using the Sievers NOA to evaluate the photolability

DOI: 10.1021/acsomega.9b00592
ACS Omega 2019, 4, 9181−9187

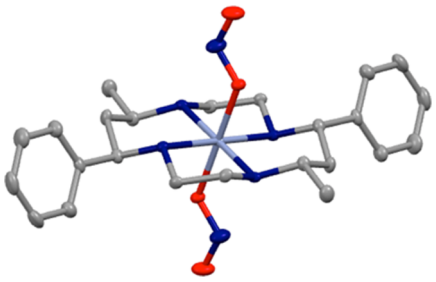

Figure 1. Structure (thermal ellipsoids at 50% probability, H atoms omitted for clarity) of one of two *trans*-Cr(PetA)$(ONO)_2^+$ cations in the independent unit determined by X-ray diffraction of [*trans*-Cr(PetA)$(ONO)_2$]BF_4 recrystallized from dichloromethane (DCM). One DCM molecule of crystallization was also found in this unit (see the packing diagram, SI Figure S5). The bond lengths and angles for both cations are provided in the Supporting Information (Table S1).

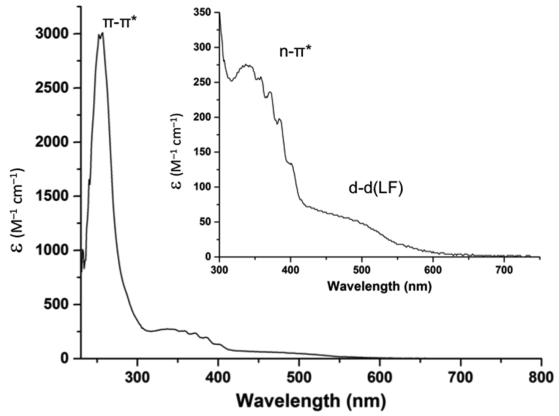

Figure 2. Absorption spectrum of [*trans*-Cr(PetA)$(ONO)_2$]BF_4 in acetonitrile solution. The λ_{max} (ε) values are 257 nm (3008 M^{-1} cm^{-1}), 337 nm (276 M^{-1} cm^{-1}), and 491 nm (51 M^{-1} cm^{-1}).

of this photoNORM toward NO release. The NOA determines with high sensitivity and precision the NO that is swept from the photolysis solution with an entraining gas (either He or medical-grade air). For PetACrONO, photoactivated NO release was readily apparent as has been shown previously for the photolysis of *trans*-Cr(cyclam)$(ONO)_2^+$ ("CrONO", cyclam = 1,4,8,11-tetraaza-cyclotetradecane). Earlier studies showed CrONO to undergo reversible CrO−NO bond homolysis to give NO and a Cr(IV) intermediate (eq 1) that can be trapped by various oxidants or reductants.[43] Quantum yields of NO release (Φ_{NO}) were relatively insensitive to excitation wavelength over the range of 365−436 nm with values in the range of 0.18−0.28 over various conditions.[44] Photolysis at 546 nm gave comparable photochemistry, despite the very low extinction coefficients at this wavelength

$$\textit{trans}\text{-Cr(cyclam)}(ONO)_2^+ \xrightleftharpoons[k_{NO}]{h\nu} \textit{trans}\text{-Cr(cyclam)}(ONO)(O)^+ + NO$$

Similarly, 451 nm photolysis of an isobutyronitrile solution of PetACrONO (0.5 mM) led to NO release as detected with the NOA. Medical-grade air was the entraining gas, and the quantitative analysis of the NO released during short defined photolysis intervals gave a Φ_{NO} value of 0.32 ± 0.01 (Figure S3), indicating that the photochemistry and photolability of the *trans*-Cr(PetA)$(ONO)_2^+$ cation are comparable to those of CrONO itself.[44] Thus, the introduction of phenyl and methyl groups to the cyclam ring and switching to a less polar medium did not inhibit the overall photolability of PetACrONO toward NO release. Analogous photolysis of PetACrONO in acetonitrile solvent using 365 nm excitation gave a similar result (Φ_{NO} = 0.30 ± 0.01).

Visible-Range Photochemistry of Loaded Polymer Disks. The above experiments demonstrated that **1** is photolabile toward NO release in fluid media. However, the question remains whether this photolability would lead to ready NO release from the PDs infused with PetACrONO. To address this point, a series of PDs were prepared from different commercial silicone-based polymer formulations (NuSil) and were infused with PetACrONO using the highly self-consistent procedures described in the Experimental Section. The silicone polymers used to fabricate the PDs are proprietorial, commercial formulations currently in use for in vivo biomedical applications. These proprietary biocompatible formulations may include different quantities of monomers, cross-linkers, resins, silica, processing aids, fillers, inhibitors, and catalysts that are designed to control the desired properties such as appearance, optical clarity, viscosity, specific gravity, tensile and tear strengths, gas permeability, etc. In all of the cases, the polymer disks appeared to be optically clear or translucent.

Photolysis studies were carried out using visible light excitation with a royal blue LED operating at 451 nm for PDs loaded only with [*trans*-Cr(PetA)$(ONO)_2$]BF_4 or using NIR excitation with a diode laser operating at 794 nm for PDs loaded both with this photoNORM and with the Nd-UCNPs. Figure 3 illustrates the NOA signals recorded for the 451 nm

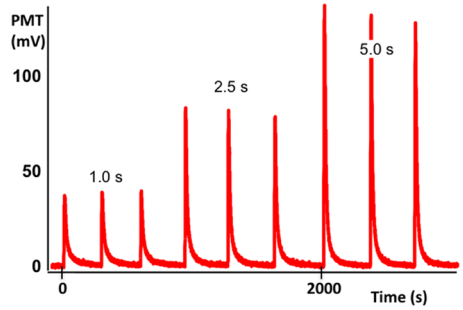

Figure 3. NOA data for 451 nm photolysis (45 mW) of silicone MED-6233 infused with [*trans*-Cr(PetA)$(ONO)_2$]BF_4 for photolysis intervals of 1.0, 2.5, and 5.0 s. The net amount of NO released from the disk was calculated from the integrated NOA signals.

LED photolysis of a PetACrONO-infused PD prepared from NuSil Technology Med-6233 for excitation times of 1.0, 2.5, and 5.0 s at 45 mW. The integrated signals provide a quantitative evaluation of the NO released in each case, the average values being 119 ± 9, 193 ± 4, and 272 ± 10 pmol, respectively. Although the longer photolysis times led to larger integrated signals, the increase was not linear. This nonlinearity may reflect the reversibility of the photoreaction in analogy to eq 1. Given that the diffusion of NO out of the polymer is relatively slow (see below), the back-reaction with the Cr(IV) oxo intermediate as in eq 1 may deplete the net amount of NO released from the PD and thus lower the photochemical efficiency. A similar pattern was observed for 451 nm photolyses of PDs prepared from the other silicone formulations infused with [*trans*-Cr(PetA)$(ONO)_2$]BF_4 (SI Table S4). In addition, successive experiments, showed a

DOI: 10.1021/acsomega.9b00592
ACS Omega 2019, 4, 9181−9187

modest decrease in the quantity of NO released, suggesting some depletion of the PetACrONO present in the PDs, which on the average totaled ∼1.7 μmol.

Close examination of the individual signals shown in Figure 3 indicates that upon 451 nm excitation of the infused PD for a period from 1.0 to 5.0 s, there is a rise of the NOA signal for several seconds, reflecting, in part, the response time of the apparatus shown in Figure S1. This is followed by a decay of the signal that fits reasonably well to a single exponential decay function (Figure 4). For example, the NOA signal decay

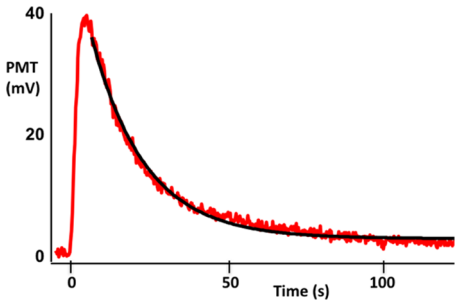

Figure 4. Temporal signal from the NOA upon 451 nm photolysis of the PetACrONO in a silicone MED-6233 PD for 1.0 s, showing a fit of the signal decay of the NOA signal fit to a first-order exponential.

subsequent to a 1.0 s irradiation of PetACrONO infused in a Med-6233 PD displayed an average lifetime (τ_{decay}) of 17.0 ± 0.3 s (Figure 4), and this was reproducible for subsequent 1 s excitations within the experimental uncertainty given. Similar decays were observed for the 2.5 and 5.0 s irradiation periods of the same sample, although the fits gave somewhat smaller values of τ_{decay}, 14.1 ± 0.2 and 12.3 ± 0.1 s, respectively. As would be expected, these decay properties are a property of the specific silicone formulation utilized to prepare the PDs, although the differences in the calculated τ_{decay} values are not dramatic. These data are presented in SI Figures S7−S9 and SI Table S5, with τ_{decay} values ranging from 14 to 28 s with samples excited for 1.0 s and with similar ranges (∼12−22 and ∼11−19 s, respectively) for excitation times of 2.5 and of 5.0 s. A logical explanation for the decay lifetimes would be that they represent diffusion to the surface of the NO released by photoexcitation of PetACrONO at a collection of different accessible sites within the polymer matrix. Given the heterogeneity of these devices, there is no reason to expect strictly exponential decays, despite the apparent shapes of these curves.

NIR Photochemistry of Loaded Polymer Disks. Figure 5 demonstrates the overlap between the emission from Nd-UCNPs upon 794 nm excitation and the absorption spectrum of PetACrONO. The upconverted visible emission from these Nd-UCNPs is readily apparent in SI Figure S10, which illustrates the result of passing a beam of 794 nm light through a hexane solution containing this material. PDs from single polymer formulation, NuSil Technology Med-6019, were used for these studies given the relatively modest differences in the photochemical properties of the PetACrONO-loaded PDs summarized in SI Tables S4 and S5.

Figure 6 displays the NOA signals observed upon 794 nm excitation of Med-6019 PDs loaded with PETACrONO and with the Nd-UCNPs. NO release that increases with increasing laser power is readily apparent. The averaged integrated NOA signals demonstrate the release of 26.4, 56.6, 88.7, and 110.3

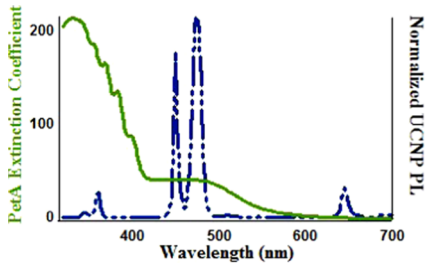

Figure 5. Comparison of the absorption spectrum of *trans*-$[Cr(PetA)(ONO)_2]BF_4$ in acetonitrile (green line) to the photoluminescence spectrum of the Nd/Tm-UCNP: β-$NaYF_4$:Tm/Nd/Yb/Gd-(0.5/1.0/30/20%)@ $NaGdF_4$:Tm(20%) upon 794 nm excitation with the laser power 1100 mW (blue).

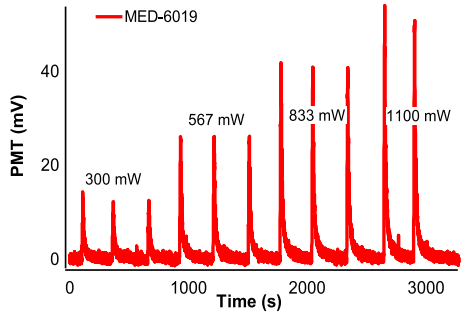

Figure 6. NOA signals for 10 s photolyses of *trans*-$[Cr(PetA)(ONO)_2]BF_4$ infused into a MED-6019 PD at 794 nm with different diode laser powers.

pmol of NO for excitations at 300, 567, 833, and 1100 mW, respectively. No nitric oxide was released upon 794 nm irradiation of a PD loaded only with PETACrONO; so, this behavior can readily be attributed to the presence of the Nd-UCNPs. The NO release proved to be almost linear with the laser power employed, and this proved somewhat unexpected given the nonlinear behavior seen for aqueous solutions containing the photoNORM RBS ($Na[Fe_4S_3(NO)_7]$) and silica-coated $NaYF_4$:Yb/Er@$NaYF_4$ core/shell UCNPs that are activated with 980 nm excitation.[39] However, as noted above, direct excitation at 451 nm did not respond linearly to irradiation time, and this was attributed to enhanced back-reactions when more NO was generated in a single event. Thus, two counteracting trends may be at play in the present case.

SUMMARY

In these studies, we report the synthesis and characterization of a new lipid-soluble photoNORM, the chromium(III) *O*-nitrito complex salt *trans*-$[Cr(PetA)(ONO)_2]BF_4$. Visible light excitation of silicone polymer disks prepared from various biocompatible commercial formulations triggers the release of NO in quantities determined by the length of the excitation pulse. Thus, photouncaging from such an implantable device allows one to define the location, timing, and dosage for the release of this potent bioregulator. However, with the exception of a subcutaneous implant, such a device would need to be attached to an optical fiber owing to the relatively poor tissue transmission of visible light. To address this issue, we also report that including neodymium-doped β-$NaYF_4$:Tm/Nd/Yb/Gd@$NaYF_4$:Nd, upconverting nanoparticles in the polymer disk allows the use of much more

DOI: 10.1021/acsomega.9b00592
ACS Omega 2019, 4, 9181−9187

penetrating NIR wavelengths at ~800 nm as the excitation source. NIR photoexcitation of these UCNPs leads to the emission of upconverted visible light and activates NO release from the photoNORM. The mechanism of such photosensitization has not been determined, although it is likely that this occurs by "trivial" energy transfer, namely, the emission of light from the UCNP followed by reabsorption by the photoNORM.

The above studies represent a continuation of our earlier demonstration of NO uncaging by 980 nm photoexcitation of poly(dimethylsiloxane) PDs containing the RBS as the photoNORM and β-$NaYF_4$:Er/Yb/Gd@$NaYF_4$ UCNPs as the NIR activator.[33] Although the latter investigation showed that such NIR photoactivation could indeed be effected through tissue filters, the inclusion of Nd^{3+} in the core and shell of the Nd-UCNPs used here allows the application of 794 nm excitation and thus avoids potential heat damage owing to the modest absorbance by water at 980 nm.[42]

We had anticipated that the different commercial formulations of the silicone polymers might lead to considerable differences in performance with regard to NO uncaging. However, the differences are relatively small, with both the quantity and τ_{decay} for NO release upon a short-term (e.g., 1 s) excitation varying only about a factor of 2 for the various formulations (SI Tables S4 and S5). This similarity may, in part, be due to each of these formulations being silicone-based but also is likely the result of the photoNORM being infused into preformed PDs as opposed to being codissolved prior to the gelling process. As a result, this precursor is located at readily accessible sites where NO once uncaged can diffuse to the surface. In contrast, Ostrowski and co-workers prepared similarly sized films of composites but dissolved their photoNORM in the polymers prior to curing, resulting in marked differences in release efficiencies depending on the gas permeabilities of the materials involved.[30]

■ ASSOCIATED CONTENT

Supporting Information

The Supporting Information is available free of charge on the ACS Publications website at DOI: 10.1021/acsomega.9b00592.

Detailed procedures for the syntheses of the PetA chromium(III) complexes and for the preparation of polymer disks; crystal structure details for *trans*-[Cr(PetA)$(ONO)_2$]BF_4, *trans*-[Cr(PetA)Cl_2]Cl, and *cis*-[Cr(PetA)Cl_2]Cl as well as 10 figures and 6 tables (PDF)

CIF files for the three crystal structures reported (CIF) (CIF) (CIF)

■ AUTHOR INFORMATION

Corresponding Author

*E-mail: ford@chem.ucsb.edu.

ORCID

Peter C. Ford: 0000-0002-5509-9912

Present Address

‡P.-J. Huang, email: po-ju.huang@agilent.com; J. V. Garcia, email: john_g95134@yahoo.com; and A. Fenwick, email: afenwick@caltech.edu.

Author Contributions

†P.J.H., J.V.G., and A.F. contributed equally to the experimental studies.

Funding

This work was supported, in part, by the Chemistry Division of the National Science Foundation (Grants CHE-1405062 and CHE-1565702).

Notes

The authors declare no competing financial interest.

■ ACKNOWLEDGMENTS

The authors thank the Molecular Foundry User Program, especially Dr. Emory Chan and Elizabeth S. Levy of the Molecular Foundry (supported by the Office of Science, Office of Basic Energy Sciences, US Department of Energy under Contract no. DE-AC02-05CH11231), for the synthesis of UCNPs. J.V.G. thanks the PIRE-ECCI (Grant NSF-OISE-0968399) program at UCSB for graduate fellowships. This research was partially supported by a grant from the National Science Foundation (CHE-1565702). The authors thank Dr. Jerry Macala of Allergan Medical and Jack Lambert of NuSil Technology for providing medical-grade silicone formulations and for technical assistance. Bruce Dunson of UCSB fabricated molds to make silicone disks and Richard Bock helped design and build glassware for the photolysis apparatus.

■ REFERENCES

(1) Smith, N. A.; Sadler, P. J. Photoactivatable metal complexes: from theory to applications in biotechnology and medicine. *Philos. Trans. R. Soc. A* **2013**, *371*, No. 20120519.

(2) Pierri, A. E.; Muizzi, D. A.; Ostrowski, A. D.; Ford, P. C. Photocontrolled release of NO and CO with inorganic and organometallic complexes. *Struct. Bonding* **2015**, *165*, 1−45.

(3) Diring, S.; Carne-Sanchez, A.; Zhang, J.; Ikemura, S.; Kim, C.; Inaba, H.; Kitagawa, S.; Furukawa, S. Light responsive metal-organic frameworks as controllable CO-releasing cell culture substrates. *Chem. Sci.* **2017**, *8*, 2381−2386.

(4) Li, A.; Turro, C.; Kodanko, J. J. Ru(II) polypyridyl complexes as photocages for bioactive compounds containing nitriles and aromatic heterocycles. *Chem. Commun.* **2018**, *54*, 1280−1290.

(5) Soboleva, T.; Esquer, H. J.; Anderson, S. N.; Berreau, L. M.; Benninghoff, A. D. Mitochondrial-Localized Versus Cytosolic Intracellular CO-Releasing Organic PhotoCORMs: Evaluation of CO Effects Using Bioenergetics. *ACS Chem. Biol.* **2018**, *13*, 2220−2228.

(6) Heinemann, F.; Karges, J.; Gasser, G. Critical Overview of the Use of Ru(II) Polypyridyl Complexes as Photosensitizers in One-Photon and Two-Photon Photodynamic Therapy. *Acc. Chem. Res.* **2017**, *50*, 2727−2736.

(7) Filevich, O.; Zayat, L.; Baraldo, L. M.; Etchenique, R. Long Wavelength Phototriggering: Ruthenium-Based Caged Compounds. *Struct. Bonding* **2015**, *165*, 47−68.

(8) Anderson, E. D.; Gorka, A. P.; Schnermann, M. J. Near-infrared uncaging or photosensitizing dictated by oxygen tension. *Nat. Commun.* **2016**, *7*, No. 13378.

(9) Agarwal, H. K.; Janicek, R.; Chi, S.-H.; Perry, J. W.; Niggli, E.; Ellis-Davies, G. C. R. Calcium Uncaging with Visible Light. *J. Am. Chem. Soc.* **2016**, *138*, 3687−3693.

(10) See, E. M.; Peck, C. L.; Guo, X.; Santos, W.; Robinson, H. D. Plasmon-Induced Photoreaction of o-Nitrobenzyl-Based Ligands under 550 nm Light. *J. Phys. Chem. C* **2017**, *121*, 13114−13124.

(11) Askes, S. H. C.; Reddy, G. U.; Wyrwa, R.; Bonnet, S.; Schiller, A. Red Light-Triggered CO Release from Mn-2(CO)(10)Using Triplet Sensitization in Polymer Nonwoven Fabrics. *J. Am. Chem. Soc.* **2017**, *139*, 15292−15295.

(12) Ignarro, L. J., Freeman, B. A., Ed. *Nitric Oxide: Biology and Pathobiology*, 3rd ed.; Elsevier Inc.: Burlington, MA, 2017.

DOI: 10.1021/acsomega.9b00592
ACS Omega 2019, 4, 9181−9187

(13) Heinrich, T. A.; da Silva, R. S.; Miranda, K. M.; Switzer, C. H.; Wink, D. A.; Fukuto, J. M. Biological nitric oxide signalling: chemistry and terminology. *Brit. J. Pharmocol.* **2013**, *169*, 1417−1429.
(14) Arora, D. P.; Hossain, S.; Xu, Y.; Boon, E. M. Nitric Oxide Regulation of Bacterial Biofilms. *Biochemistry* **2015**, *54*, 3717−3728.
(15) Ford, P. C. Photochemical delivery of nitric oxide. *Nitric Oxide* **2013**, *34*, 56−64.
(16) Evans, M. A.; Huang, P.-J.; Iwamoto, Y.; Ibsen, K. N.; Chan, E. M.; Hitomi, Y.; Ford, P. C.; Mitragotri, S. Macrophage-Mediated Delivery of Light Activated Nitric Oxide Prodrugs with Spatial, Temporal and Concentration Control. *Chem. Sci.* **2018**, *9*, 3729−3741.
(17) Ford, P. C. Metal complex strategies for photo-uncaging the small molecule bioregulators nitric oxide and carbon monoxide. *Coord. Chem. Rev.* **2018**, *376*, 548−564.
(18) deBoer, T. R.; Mascharak, P. K. Recent Progress in Photoinduced NO Delivery with Designed Ruthenium Nitrosyl Complexes. *Adv. Inorg. Chem.* **2015**, *67*, 145−170.
(19) Fraix, A.; Sortino, S. Combination of PDT photosensitizers with NO photodononors. *Photochem. Photobiol. Sci.* **2018**, *17*, 1709−1727.
(20) Conte, C.; Fraix, A.; Thomsen, H.; Ungaro, F.; Cardile, V.; Graziano, A. C. E.; Ericson, M. B.; Quaglia, F.; Sortino, S. Monitoring the release of a NO photodonor from polymer nanoparticles via Forster resonance energy transfer and two-photon fluorescence imaging. *J. Mater. Chem. B* **2018**, *6*, 249−256.
(21) Rodrigues, F. P.; Carneiro, Z. A.; Mascharak, P.; Curti, C.; da Silva, R. S. Incorporation of a ruthenium nitrosyl complex into liposomes, the nitric oxide released from these liposomes and HepG2 cell death mechanism. *Coord. Chem. Rev.* **2016**, *306*, 701−707.
(22) Xiang, H.-J.; Guo, M.; Liu, J.-G. Transition-Metal Nitrosyls for Photocontrolled Nitric Oxide Delivery. *Eur. J. Inorg. Chem.* **2017**, *12*, 1586−1595.
(23) Hitomi, Y.; Iwamoto, Y.; Kodera, M. Electronic Tuning of Nitric Oxide Release from Manganese Nitrosyl Complexes by Visible Light Irradiation: Enhancement of Nitric Oxide Release Efficiency by the Nitro-Substituted Quinoline Ligand. *Dalton Trans.* **2014**, *43*, 2161−2167.
(24) Guo, R. R.; Tian, Y.; Wang, Y.; Yang, W. Near-Infrared Laser-Triggered Nitric Oxide Nanogenerators for the Reversal of Multidrug Resistance in Cancer. *Adv. Funct. Mater.* **2017**, *27*, No. 1606398.
(25) Tfouni, E.; Truzzi, D. R.; Tavares, A.; Gomes, A. J.; Figueiredo, L. E.; Franco, D. W. Biological activity of ruthenium nitrosyl complexes. *Nitric Oxide* **2012**, *26*, 38−53.
(26) Smith, A. M.; Mancini, M. C.; Nie, S. Second window for in vivo imaging. *Nat. Nanotechnol.* **2009**, *4*, 710−711.
(27) Frost, M. C.; Reynolds, M. M.; Meyerhoff, M. E. Polymers incorporating nitric oxide releasing/generating substances for improved biocompatibility of blood-contacting medical devices. *Biomaterials* **2005**, *26*, 1685−1693.
(28) Tfouni, E.; Bordini, J.; Ford, P. C. Photochemical release of nitric oxide from a regenerable $[Ru(salen)(H_2O)(NO)]^+$ via sol-gel chemistry. *Chem. Commun.* **2005**, 4169−4171.
(29) Nichols, S. P.; Storm, W. L.; Koh, A.; Schoenfisch, M. H. Local delivery of nitric oxide: Targeted delivery of therapeutics to bone and connective tissues. *Adv. Drug Delivery Rev.* **2012**, *64*, 1177−1188.
(30) Mase, J. D.; Razgoniaev, A. O.; Tschirhart, M. K.; Ostrowski, A. D. Light-controlled release of nitric oxide from solid polymer composite materials using visible and near infra-red light. *Photochem. Photobiol. Sci.* **2015**, *14*, 777−785.
(31) Wolinsky, J. B.; Colson, Y. L.; Grinstaff, M. W. Local drug delivery strategies for cancer treatment: Gels, nanoparticles, polymeric films, rods, and wafers. *J. Controlled Release* **2012**, *159*, 14−26.
(32) Timko, B. P.; Arruebo, M.; Shankarappa, S. A.; McAlvin, J. B.; Okonkwo, O. S.; Mizrahi, B.; Stefanescu, C. F.; Gomez, L.; Zhu, J.; Zhu, A.; Santamaria, J.; Langer, R.; Kohane, D. S. Near-infrared−actuated devices for remotely controlled drug delivery. *Proc. Natl. Acad. Sci. USA* **2014**, *111*, 1349−1354.
(33) Burks, P. T.; Garcia, J. V.; GonzalezIrias, R.; Tillman, J. T.; Niu, M.; Mikhailovsky, A. A.; Zhang, J.; Zhang, F.; Ford, P. C. Nitric Oxide Releasing Materials Triggered by Near-Infrared Excitation Through Tissue Filter. *J. Am. Chem. Soc.* **2013**, *135*, 18145.
(34) Garcia, J. V.; Zhang, F.; Ford, P. C. Multi-Photon Excitation in Uncaging the Small Molecule Bioregulator Nitric Oxide. *Philos. Trans. R. Soc. A* **2013**, *371*, No. 20120129.
(35) Chan, E. M.; Levy, E. S.; Cohen, B. E. Rationally Designed Energy Transfer in Upconverting Nanoparticles. *Adv. Mater.* **2015**, *27*, 5753−576.
(36) Ruggiero, E.; Alonso-de Castro, S.; Habtemariam, A.; Salassa, L. Upconverting nanoparticles for the near infrared photoactivation of transition metal complexes: new opportunities and challenges in medicinal inorganic photochemistry. *Dalton Trans.* **2016**, *45*, 13012−13020.
(37) Wu, S.; Blinco, J. P.; Barner-Kowollik, C. Near-Infrared Photoinduced Reactions Assisted by Upconverting Nanoparticles. *Chem. Eur. J.* **2017**, *23*, 8325−8332.
(38) Pierri, A. E.; Huang, P.-J.; Garcia, J. V.; Stanfill, J. G.; Chui, M.; Wu, G.; Zheng, N.; Ford, P. C. A photoCORM nanocarrier for CO release using NIR light. *Chem. Commun.* **2015**, *51*, 2072−2075.
(39) Garcia, J. V.; Yang, J.; Shen, D.; Yao, C.; Li, X.; Stucky, G. D.; Zhao, D. Y.; Ford, P. C.; Zhang, F.; et al. Near-Infrared Triggered Release of Caged Nitric Oxide using Upconversion Nanostructured Materials. *Small* **2012**, *8*, 3800−3805.
(40) Inclusion of the Gd^{3+} in the formulation of UCNPs was for synthetic convenience since the only function is to facilitate formation of the hexagonal phase of $NaYF_4$ (ref 41). Given the toxicity of gadolinium salts, extensions of such studies to in vivo experiments would utilize other procedures to achieve the same purpose.
(41) Ostrowski, A. D.; Chan, E. M.; Gargas, D. J.; Katz, E. M.; Han, G.; Schuck, P. J.; Milliron, D. J.; Cohen, B. E. Controlled Synthesis and Single-Particle Imaging of Bright, Sub-10 nm Lanthanide-Doped Upconverting Nanocrystals. *ACS Nano* **2012**, *6*, 2686−2692.
(42) Xie, X.; Gao, N.; Deng, R.; Sun, Q.; Xu, Q.-H.; Liu, X. Mechanistic Investigation of Photon Upconversion in Nd^{3+} Sensitized Core −Shell Nanoparticles. *J. Am. Chem. Soc.* **2013**, *135*, 12608−12611.
(43) Shen, J.; Chen, G.; Vu, A.-M.; Fan, W.; Bilsel, O. S.; Chang, C.-C.; Han, G. Engineering the Upconversion Nanoparticle Excitation Wavelength: Cascade Sensitization of Tri-doped Upconversion Colloidal Nanoparticles at 800 nm. *Adv. Opt. Mater.* **2013**, *1*, 644−650.
(44) De Leo, M. A.; Ford, P. C. Reversible Photolabilization of NO from Chromium(III) Coordinated Nitrite. A New Strategy for Nitric Oxide Delivery. *J. Am. Chem. Soc.* **1999**, *121*, 1980−1981.
(45) Ostrowski, A. D.; Absalonson, R. O.; De Leo, M. A.; Wu, G.; Pavlovich, J. G.; Adamson, J.; Azhar, B.; Iretskii, A. V.; Megson, I. L.; Ford, P. C. The Photochemistry of *trans*-$Cr(cyclam)(ONO)_2^+$, a Nitric Oxide Precursor. *Inorg. Chem.* **2011**, *50*, 4453−4462.
(46) Hideg, K.; Lloyd, D. Reaction Products from Unsaturated Ketones and Aliphatic Diamines or Dithiols. *J. Chem. Soc. C* **1971**, 3441−3445.
(47) DeRosa, F.; Bu, X.; Pohaku, K.; Ford, P. C. Synthesis and photophysical properties of Cr(III) complexes with cyclam-type ligands having pendant chromophores, *trans*-$[Cr(L)Cl_2]Cl$. *Inorg. Chem.* **2005**, *44*, 4166−4174.

DOI: 10.1021/acsomega.9b00592
ACS Omega 2019, 4, 9181−9187